A Stochastic Design Approach for Iterative Learning Observers for the Estimation of Periodically Recurring Trajectories and Disturbances

Andreas Rauh, Thomas Chevet, Thach Ngoc Dinh, Julien Marzat, Tarek Raissi

A Stochastic Design Approach for Iterative Learning Observers for the Estimation of Periodically Recurring Trajectories and Disturbances

Andreas Rauh[1], Thomas Chevet[2], Thach Ngoc Dinh[3], Julien Marzat[2], and Tarek Raïssi[3]

Abstract— **Many repetitive control problems are characterized by the fact that disturbances have the same effect in each successive execution of the same control task. Such disturbances comprise the lumped representation of unmodeled parts of the open-loop system dynamics, a systematic model-mismatch or, more generally, deterministic yet unknown uncertainty. In such cases, well-known strategies for iterative learning control are based on enhancing the system behavior not only by exploiting data gathered during a single execution of the task but also using information from previous executions. The corresponding dual problem, namely, iterative learning state and disturbance estimation has not yet received the same amount of attention. However, it is obvious that improved estimates for the aforementioned states and disturbances which periodically occur in each execution will be a means to achieve an improved accuracy and, therefore, in future work also to optimize the control accuracy. In this paper, we present a joint design procedure for observer gains in two independent dimensions, a gain for processing information in the temporal domain during a single execution of the task (also named trial) and a gain for learning in the iteration domain (i.e., from trial to trial).**

I. Introduction

Two-dimensional (2D) systems with the time domain and the iteration domain as two independent dimensions have been widely used in the last decades to derive iterative learning control (ILC) procedures [1]–[3]. Such approaches can be applied effectively for enhancing the control accuracy of repetitive tasks that are characterized by identical reference trajectories of finite length during each successive execution of a control task, where before the restart of the execution a reset to (nearly) the same initial conditions takes place. Such tasks occur widely in pick and place operations of manufacturing processes as well as during welding executed by robots. They can also be found in other areas such as rehabilitation or the control of wind power plants. ILC has the unique feature that it does not only exploit past data that are classically available in control tasks from the current execution of the task under consideration. In addition, it also exploits information from previous evaluations and is hence able to outperform control implementations that only exploit current trial data. By using information from one or multiple previous trials, control structures can be implemented which classically would even be acausal.

The dual task of iterative learning observer (ILO) synthesis [4] has not yet achieved the same amount of attention. Related work can be found in [5], where a Kalman Filter (KF) [6] like ILO procedure is derived for the time and iteration domains. However, the drawback of the approach proposed in [5] is its suboptimality because both independent domains are treated separately. This problem was removed by deriving a linear matrix inequality (LMI) design approach for a learning-based observer for linear discrete-time dynamics with uncertain temporally varying parameters in [7]. The structure of this observer is motivated by the work of [8]. It yields point-valued state as well as disturbance estimates and includes a strategy for identifying a constant, but not perfectly known initial system state. For nonlinear applications, data-driven learning observer approaches were derived in [9], [10]. Recently, a related topic in the frame of an interval observer design for 2D systems described in the form of the Fornasini-Marchesini second model was derived in [11], where the focus was on evaluating and verifying stability criteria in the form of LMIs in combination with the optimization of the peak-to-peak norm to reduce the effects of measurement errors on the state estimates.

In this paper, we focus on deriving a novel stochastic ILO approach for linear time-varying system models, which aims at minimizing (as in the case of a classical KF) the estimation error covariance. In contrast to the existing work in [5], we do not search for a suboptimal solution by computing the observer gains in the time and iteration domains independently but rather compute them jointly with the help of a closed-form expression. For that purpose, it is only required to specify the discrete-time state-space representation of the system under consideration together with the physically motivated covariance matrices of process and sensor noise.

This paper is structured as follows. In Sec. II, we describe the problem formulation of ILO design for linear discrete-time, time-varying system models. Sec. III proposes the closed-form solution of the observer design problem before simulation results are presented for a close-to-life battery model in Sec. IV. Finally, conclusions and an outlook on future work can be found in Sec. V.

Notation: Throughout this paper, $\mathbf{I}$ and $\mathbf{0}$ denote identity and zero matrices of appropriate dimensions; $\mathrm{tr}(\mathbf{A})$ is the trace (sum of diagonal elements) of a square matrix; $k \in \{0, \ldots, k_{\max}\}$ denotes the discrete time index and $i \in \mathbb{N}_0$ is a non-negative integer counter for the iteration (trial) number;

[1]A. Rauh is with Carl von Ossietzky Universität Oldenburg, Department of Computing Science, Group: Distributed Control in Interconnected Systems, D-26111 Oldenburg, Germany. Andreas.Rauh@uni-oldenburg.de

[2]T. Chevet and J. Marzat are with DTIS, ONERA, Université Paris-Saclay, 91123 Palaiseau, France. {thomas.chevet, julien.marzat}@onera.fr

[3]T.N. Dinh and T. Raïssi are with Conservatoire National des Arts et Métiers (CNAM), Cedric-Laetitia, 292 Rue St-Martin, 75141, Paris Cedex 03, France. ngoc-thach.dinh@lecnam.net, tarek.raissi@cnam.fr

the symbol $\star$ indicates blocks in symmetric matrices that can be inferred from the remaining elements by a transposition.

II. Problem Formulation

Consider the linear discrete-time state-space representation

$$\begin{aligned}\mathbf{x}_{k+1} &= \mathbf{A}_k \cdot \mathbf{x}_k + \mathbf{E}_k \cdot \mathbf{w}_k \\ \mathbf{y}_k &= \mathbf{C}_k \cdot \mathbf{x}_k + \mathbf{v}_k\end{aligned} \tag{1}$$

with the state vector $\mathbf{x}_k \in \mathbb{R}^n$, the potentially time-varying system, disturbance input, and output matrices $\mathbf{A}_k$, $\mathbf{E}_k$, and $\mathbf{C}_k$, respectively, and process and measurement noise vectors $\mathbf{w}_k$ and $\mathbf{v}_k$, which are both assumed to be normally distributed with the covariances $\mathbf{C}_{\mathbf{w},k}$ and $\mathbf{C}_{\mathbf{v},k}$ and vanishing mean. The goal of this paper is to estimate the state vector as well as its uncertainty by a KF-like procedure that does not only operate along the time domain k but also enhances the estimates over subsequent evaluations of the system model, i.e., from the trial i to the trial $i+1$, by considering a lumped correction term $\boldsymbol{\delta}_k$ added to the state equations in the form

$$\mathbf{x}_{k+1} = \mathbf{A}_k \cdot \mathbf{x}_k + \mathbf{E}_k \cdot \mathbf{w}_k + \boldsymbol{\delta}_k \tag{2}$$

so that the deterministic mismatch of the dynamics represented by the model (1) and the real-life system behavior can be approximated. This model mismatch is estimated on the basis of the actually measured data $\mathbf{y}^{\xi}_{\mathrm{m},k} = \mathbf{C}^{\xi}_k \cdot \mathbf{x}^{\xi}_k + \mathbf{v}^{\xi}_k$ during the trials $\xi = i$ and $\xi = i+1$, denoting the realizations of the general system output $\mathbf{y}_k$ in (1). In such a way, the estimate for the temporal evolution of $\boldsymbol{\delta}_k$ is refined before starting the next trial.

Remark: As in the case of a classical Extended Kalman Filter (EKF), the system model (1) can represent a time-varying and/or quasi-linear or linearized system model in the form

$$\begin{aligned}\mathbf{x}_{k+1} &= \mathbf{A}_k(\tilde{\mathbf{x}}_k) \cdot \mathbf{x}_k + \mathbf{E}_k(\tilde{\mathbf{x}}_k) \cdot \mathbf{w}_k \\ \mathbf{y}_k &= \mathbf{C}(\tilde{\mathbf{x}}_k) \cdot \mathbf{x}_k + \mathbf{v}_k \ ,\end{aligned} \tag{3}$$

where $\tilde{\mathbf{x}}_k$ represents the most recent state estimate, so that $\mathbf{A}_k := \mathbf{A}_k(\tilde{\mathbf{x}}_k)$, $\mathbf{E}_k := \mathbf{E}_k(\tilde{\mathbf{x}}_k)$, and $\mathbf{C}_k := \mathbf{C}_k(\tilde{\mathbf{x}}_k)$ hold.

Remark: In the system models (1) and (3), control inputs are not explicitly included. However, if a system is actually non-autonomous, and the inputs are known exactly, the design procedure presented in the following section with its gain computation remains unchanged because all covariance matrices are independent of this system input. This is in full analogy to the case of a classical KF design which only operates along the time domain and would not make use of the trial-to-trial update presented in this paper.

III. Design of the Stochastic ILO Scheme

As already mentioned in the previous section, we assume in this paper that process and measurement noise are uncorrelated and normally distributed with zero mean. In all of the following equations, the superscript p denotes the result of the prediction step, while the superscript e refers to the estimation result as the outcome of the measurement-based innovation step.

A. Prediction Step

The ILO design is essentially based on the standard detectability requirement known from the KF synthesis. If this is satisfied, assume that two gain matrices $\mathbf{H}^{i+1}_{1,k}$ and $\mathbf{H}^{i+1}_{2,k}$ are included in the observer, where the first one serves as a KF-like stabilization along the trial and the latter allows for reducing estimation errors between two subsequent trials. As a general index convention, use the index i to denote the old trial for which the state estimation has already been performed previously and $i+1$ denotes the current trial. To design the gains for the trial $i+1$, an augmented system model containing the models for the i-th and $(i+1)$-st trials is defined. Using this model, the expected values are updated in the prediction step by means of

$$\begin{bmatrix}\boldsymbol{\mu}^{\mathrm{p},i}_{k+1} \\ \boldsymbol{\mu}^{\mathrm{p},i+1}_{k+1}\end{bmatrix} = \begin{bmatrix}\mathbf{A}^i_k & \mathbf{0} \\ \mathbf{0} & \mathbf{A}^{i+1}_k\end{bmatrix} \cdot \begin{bmatrix}\boldsymbol{\mu}^{\mathrm{e},i}_{k} \\ \boldsymbol{\mu}^{\mathrm{e},i+1}_{k}\end{bmatrix} \ , \tag{4}$$

where $\mathbf{A}^i_k := \mathbf{A}_k\left(\boldsymbol{\mu}^{\mathrm{e},i}_k\right)$ and $\mathbf{A}^{i+1}_k := \mathbf{A}_k\left(\boldsymbol{\mu}^{\mathrm{e},i+1}_k\right)$ are the system matrices evaluated for the most recent estimation results $\boldsymbol{\mu}^{\mathrm{e},i}_k$ and $\boldsymbol{\mu}^{\mathrm{e},i+1}_k$, respectively, that are both recomputed during the trial $i+1$. This kind of evaluation of the system matrices allows for treating linearized and quasi-linear formulations in an EKF-like manner. In full analogy to the system matrices above, the disturbance input matrices are defined as $\mathbf{E}^i_k := \mathbf{E}_k\left(\boldsymbol{\mu}^{\mathrm{e},i}_k\right)$ and $\mathbf{E}^{i+1}_k := \mathbf{E}_k\left(\boldsymbol{\mu}^{\mathrm{e},i+1}_k\right)$. With their help, the covariance prediction yields

$$\begin{aligned}\mathbf{C}^{\mathrm{p},i|i+1}_{k+1} = &\begin{bmatrix}\mathbf{A}^i_k & \mathbf{0} \\ \mathbf{0} & \mathbf{A}^{i+1}_k\end{bmatrix} \cdot \mathbf{C}^{\mathrm{e},i|i+1}_{k} \cdot \begin{bmatrix}\mathbf{A}^i_k & \mathbf{0} \\ \mathbf{0} & \mathbf{A}^{i+1}_k\end{bmatrix}^T \\ &+ \begin{bmatrix}\mathbf{E}^i_k & \mathbf{0} \\ \mathbf{0} & \mathbf{E}^{i+1}_k\end{bmatrix} \cdot \begin{bmatrix}\mathbf{C}_{\mathbf{w},k} & \mathbf{0} \\ \mathbf{0} & \mathbf{C}_{\mathbf{w},k}\end{bmatrix} \cdot \begin{bmatrix}\mathbf{E}^i_k & \mathbf{0} \\ \mathbf{0} & \mathbf{E}^{i+1}_k\end{bmatrix}^T \ .\end{aligned} \tag{5}$$

B. Innovation Step

The measurement-based innovation step makes use of the deviations

$$\Delta\mathbf{y}^i_k = \mathbf{y}^i_{\mathrm{m},k} - \mathbf{C}^i_k \cdot \boldsymbol{\mu}^{\mathrm{p},i}_k \quad \text{and} \tag{6}$$

$$\Delta\mathbf{y}^{i+1}_k = \mathbf{y}^{i+1}_{\mathrm{m},k} - \mathbf{C}^{i+1}_k \cdot \boldsymbol{\mu}^{\mathrm{p},i+1}_k \tag{7}$$

between the measured data in the trials i and $i+1$, respectively, and the corresponding output forecasts based on the prediction step of the previous subsection. Using these output deviations, the expected values are updated by

$$\begin{aligned}\begin{bmatrix}\boldsymbol{\mu}^{\mathrm{e},i}_{k} \\ \boldsymbol{\mu}^{\mathrm{e},i+1}_{k}\end{bmatrix} &= \begin{bmatrix}\boldsymbol{\mu}^{\mathrm{p},i}_{k} \\ \boldsymbol{\mu}^{\mathrm{p},i+1}_{k}\end{bmatrix} + \begin{bmatrix}\mathbf{H}^{i+1}_{1,k} \cdot \Delta\mathbf{y}^i_k \\ \mathbf{H}^{i+1}_{1,k} \cdot \Delta\mathbf{y}^{i+1}_k + \mathbf{H}^{i+1}_{2,k} \cdot \left(\Delta\mathbf{y}^i_k - \Delta\mathbf{y}^{i+1}_k\right)\end{bmatrix} \\ &= \begin{bmatrix}\boldsymbol{\mu}^{\mathrm{p},i}_{k} \\ \boldsymbol{\mu}^{\mathrm{p},i+1}_{k}\end{bmatrix} + \tilde{\mathbf{H}}_k \cdot \begin{bmatrix}\mathbf{y}^i_{\mathrm{m},k} \\ \mathbf{y}^{i+1}_{\mathrm{m},k}\end{bmatrix} - \tilde{\mathbf{H}}_k \tilde{\mathbf{C}}_k \cdot \begin{bmatrix}\boldsymbol{\mu}^{\mathrm{p},i}_{k} \\ \boldsymbol{\mu}^{\mathrm{p},i+1}_{k}\end{bmatrix}\end{aligned} \tag{8}$$

and the corresponding estimation error covariance [12] by

$$\begin{aligned}\mathbf{C}^{\mathrm{e},i|i+1}_{k} &= \mathrm{E}\left\{\begin{bmatrix}\mathbf{x}^i_k - \boldsymbol{\mu}^{\mathrm{e},i}_k \\ \mathbf{x}^{i+1}_k - \boldsymbol{\mu}^{\mathrm{e},i+1}_k\end{bmatrix} \cdot \begin{bmatrix}\mathbf{x}^i_k - \boldsymbol{\mu}^{\mathrm{e},i}_k \\ \mathbf{x}^{i+1}_k - \boldsymbol{\mu}^{\mathrm{e},i+1}_k\end{bmatrix}^T\right\} \\ &= \mathrm{Cov}\left\{\begin{bmatrix}\mathbf{x}^i_k - \boldsymbol{\mu}^{\mathrm{e},i}_k \\ \mathbf{x}^{i+1}_k - \boldsymbol{\mu}^{\mathrm{e},i+1}_k\end{bmatrix}\right\}\end{aligned}$$

$$= \mathrm{Cov}\left\{ \left(\begin{bmatrix} \mathbf{I} & \mathbf{0} \\ \mathbf{0} & \mathbf{I} \end{bmatrix} - \tilde{\mathbf{H}}_k \tilde{\mathbf{C}}_k \right) \cdot \begin{bmatrix} \mathbf{x}_k^i - \boldsymbol{\mu}_k^{\mathrm{p},i} \\ \mathbf{x}_k^{i+1} - \boldsymbol{\mu}_k^{\mathrm{p},i+1} \end{bmatrix} - \tilde{\mathbf{H}}_k \cdot \begin{bmatrix} \mathbf{v}_k^i \\ \mathbf{v}_k^{i+1} \end{bmatrix} \right\}$$

$$= \mathbf{M}_k \mathbf{C}_k^{\mathrm{p},i|i+1} \mathbf{M}_k^T + \tilde{\mathbf{H}}_k \tilde{\mathbf{C}}_{\mathbf{v},k} \tilde{\mathbf{H}}_k^T \quad , \tag{9}$$

where

$$\mathbf{M}_k = \begin{bmatrix} \mathbf{I} & \mathbf{0} \\ \mathbf{0} & \mathbf{I} \end{bmatrix} - \tilde{\mathbf{H}}_k \tilde{\mathbf{C}}_k \quad . \tag{10}$$

In these expressions, the following notation is used:

- Combined output matrix

$$\tilde{\mathbf{C}}_k := \begin{bmatrix} \mathbf{C}_k^i & \mathbf{0} \\ \mathbf{0} & \mathbf{C}_k^{i+1} \end{bmatrix} \tag{11}$$

  with $\mathbf{C}_k^i := \mathbf{C}_k\left(\boldsymbol{\mu}_k^{\mathrm{p},i}\right)$ and $\mathbf{C}_k^{i+1} := \mathbf{C}_k\left(\boldsymbol{\mu}_k^{\mathrm{p},i+1}\right)$;
- Augmented filter gain matrix

$$\tilde{\mathbf{H}}_k := \begin{bmatrix} \mathbf{H}_{1,k}^{i+1} & \mathbf{0} \\ \mathbf{H}_{2,k}^{i+1} & \mathbf{H}_{1,k}^{i+1} - \mathbf{H}_{2,k}^{i+1} \end{bmatrix} \quad ; \tag{12}$$

- Augmented, trial-independent measurement noise covariance

$$\tilde{\mathbf{C}}_{\mathbf{v},k} := \begin{bmatrix} \mathbf{C}_{\mathbf{v},k} & \mathbf{0} \\ \mathbf{0} & \mathbf{C}_{\mathbf{v},k} \end{bmatrix} \quad ; \tag{13}$$

- Block partitioning of the predicted covariance

$$\mathbf{C}_k^{\mathrm{p},i|i+1} = \begin{bmatrix} \mathbf{C}_{\mathrm{A},k}^{\mathrm{p}} & \mathbf{C}_{\mathrm{B},k}^{\mathrm{p}} \\ \star & \mathbf{C}_{\mathrm{C},k}^{\mathrm{p}} \end{bmatrix} \quad ; \tag{14}$$

- Block partitioning of the residual covariance

$$\tilde{\mathbf{C}}_k \mathbf{C}_k^{\mathrm{p},i|i+1} \tilde{\mathbf{C}}_k^T + \tilde{\mathbf{C}}_{\mathbf{v},k} = \begin{bmatrix} \mathbf{C}_{\mathrm{A},k} & \mathbf{C}_{\mathrm{B},k} \\ \star & \mathbf{C}_{\mathrm{C},k} \end{bmatrix} \tag{15}$$

  for the augmented system with

$$\begin{aligned} \mathbf{C}_{\mathrm{A},k} &= \mathbf{C}_k^i \mathbf{C}_{\mathrm{A},k}^{\mathrm{p}} \mathbf{C}_k^{i\,T} + \mathbf{C}_{\mathbf{v},k} \quad , \\ \mathbf{C}_{\mathrm{B},k} &= \mathbf{C}_k^i \mathbf{C}_{\mathrm{B},k}^{\mathrm{p}} \mathbf{C}_k^{i+1\,T} \quad , \quad \text{and} \\ \mathbf{C}_{\mathrm{C},k} &= \mathbf{C}_k^{i+1} \mathbf{C}_{\mathrm{C},k}^{\mathrm{p}} \mathbf{C}_k^{i+1\,T} + \mathbf{C}_{\mathbf{v},k} \quad . \end{aligned} \tag{16}$$

Remark: Cross-correlations between the trials i and $i+1$ due to the stochastic noise are neglected in the following theorem.

Theorem 3.1 (Optimal ILO gain computation): The optimal ILO gains, in the sense of a minimization of the estimation error covariance, jointly considering the trials i and $i+1$, are given by

$$\begin{aligned} &\begin{bmatrix} \mathbf{H}_{1,k}^{i+1} & \mathbf{H}_{2,k}^{i+1} \end{bmatrix} \\ &\quad = \left[\left(\mathbf{C}_k^i \mathbf{C}_{\mathrm{A},k}^{\mathrm{p}} + \mathbf{C}_k^{i+1} \mathbf{C}_{\mathrm{C},k}^{\mathrm{p}} \right)^T \; \left(\mathbf{C}_k^i \mathbf{C}_{\mathrm{B},k}^{\mathrm{p}} - \mathbf{C}_k^{i+1} \mathbf{C}_{\mathrm{C},k}^{\mathrm{p}} \right)^T \right] \\ &\quad \cdot \begin{bmatrix} \mathbf{C}_{\mathrm{A},k} + \mathbf{C}_{\mathrm{C},k} & \star \\ \mathbf{C}_{\mathrm{B},k} - \mathbf{C}_{\mathrm{C},k} & \mathbf{C}_{\mathrm{A},k} - \left(\mathbf{C}_{\mathrm{B},k} + \mathbf{C}_{\mathrm{B},k}^T \right) + \mathbf{C}_{\mathrm{C},k} \end{bmatrix}^{-1} \quad . \end{aligned} \tag{17}$$

Proof: Optimality of the ILO gains is achieved by a minimization of the cost function

$$\begin{aligned} J = \mathrm{tr}\left(\mathbf{C}_k^{\mathrm{e},i|i+1} \right) &= \mathrm{tr}\Big(\mathbf{C}_k^{\mathrm{p},i|i+1} - \tilde{\mathbf{H}}_k \tilde{\mathbf{C}}_k \mathbf{C}_k^{\mathrm{p},i|i+1} \\ &- \mathbf{C}_k^{\mathrm{p},i|i+1} \tilde{\mathbf{C}}_k^T \tilde{\mathbf{H}}_k^T + \tilde{\mathbf{H}}_k \cdot \left(\tilde{\mathbf{C}}_k \mathbf{C}_k^{\mathrm{p},i|i+1} \tilde{\mathbf{C}}_k^T + \tilde{\mathbf{C}}_{\mathbf{v},k} \right) \cdot \tilde{\mathbf{H}}_k^T \Big) \quad . \end{aligned} \tag{18}$$

Using the expressions (9)–(16), the cost function (18) is rewritten into the form

$$\begin{aligned} J = \mathrm{tr}\Big(& \mathbf{C}_k^{\mathrm{p},i|i+1} - 2\mathbf{H}_{1,k}^{i+1} \mathbf{C}_k^i \mathbf{C}_{\mathrm{A},k}^{\mathrm{p}} - 2\mathbf{H}_{2,k}^{i+1} \mathbf{C}_k^i \mathbf{C}_{\mathrm{B},k}^{\mathrm{p}} \\ & - 2\left(\mathbf{H}_{1,k}^{i+1} - \mathbf{H}_{2,k}^{i+1} \right) \mathbf{C}_k^{i+1} \mathbf{C}_{\mathrm{C},k}^{\mathrm{p}} + \mathbf{H}_{1,k}^{i+1} \mathbf{C}_{\mathrm{A},k} \mathbf{H}_{1,k}^{i+1\,T} \\ & + \mathbf{H}_{2,k}^{i+1} \mathbf{C}_{\mathrm{A},k} \mathbf{H}_{2,k}^{i+1\,T} + \mathbf{H}_{1,k}^{i+1} \mathbf{C}_{\mathrm{B},k}^T \mathbf{H}_{2,k}^{i+1\,T} - 2\mathbf{H}_{2,k}^{i+1} \mathbf{C}_{\mathrm{B},k}^T \mathbf{H}_{2,k}^{i+1\,T} \\ & + \mathbf{H}_{2,k}^{i+1} \mathbf{C}_{\mathrm{B},k} \mathbf{H}_{1,k}^{i+1\,T} + \mathbf{H}_{1,k}^{i+1} \mathbf{C}_{\mathrm{C},k} \mathbf{H}_{1,k}^{i+1\,T} - \mathbf{H}_{1,k}^{i+1} \mathbf{C}_{\mathrm{C},k} \mathbf{H}_{2,k}^{i+1\,T} \\ & - \mathbf{H}_{2,k}^{i+1} \mathbf{C}_{\mathrm{C},k} \mathbf{H}_{1,k}^{i+1\,T} + \mathbf{H}_{2,k}^{i+1} \mathbf{C}_{\mathrm{C},k} \mathbf{H}_{2,k}^{i+1\,T} \Big) \end{aligned} \tag{19}$$

that explicitly depends on the gain matrices $\mathbf{H}_{1,k}^{i+1}$ and $\mathbf{H}_{2,k}^{i+1}$ to be determined.

With the help of the general differentiation rules

$$\begin{aligned} &\frac{\partial \mathrm{tr}\left(\mathbf{XA}\right)}{\partial \mathbf{X}} = \mathbf{A}^T \ , \quad \frac{\partial \mathrm{tr}\left(\mathbf{AX}^T\right)}{\partial \mathbf{X}} = \mathbf{A} \ , \quad \text{and} \\ &\frac{\partial \mathrm{tr}\left(\mathbf{XAX}^T\right)}{\partial \mathbf{X}} = \mathbf{X} \cdot \left(\mathbf{A} + \mathbf{A}^T \right) \ , \end{aligned} \tag{20}$$

for the matrix trace operator applied to linear and quadratic forms, and differentiating J as stated in (19) with respect to $\mathbf{H}_{1,k}^{i+1}$ and $\mathbf{H}_{2,k}^{i+1}$, the corresponding necessary optimality conditions for a minimum of the estimation error covariance are obtained by setting both derivatives to zero. Resolving these equations, which are then linear in $\mathbf{H}_{1,k}^{i+1}$ and $\mathbf{H}_{2,k}^{i+1}$, provides the closed-form expression (17) for the ILO gains. These gains correspond to the global minimum of the cost function (18) because the matrix

$$\begin{bmatrix} \mathbf{C}_{\mathrm{A},k} + \mathbf{C}_{\mathrm{C},k} & \star \\ \mathbf{C}_{\mathrm{B},k} - \mathbf{C}_{\mathrm{C},k} & \mathbf{C}_{\mathrm{A},k} - \left(\mathbf{C}_{\mathrm{B},k} + \mathbf{C}_{\mathrm{B},k}^T \right) + \mathbf{C}_{\mathrm{C},k} \end{bmatrix} \tag{21}$$

to be inverted in (17) is positive definite (ensuring uniqueness of the optimum in the sense of a minimum of J) for observable systems with proper covariance matrices. This completes the proof of Theorem 3.1. ■

C. Summary of the ILO Procedure

So far, only the prediction and innovation steps of a single evaluation of the stochastic estimation procedure were described which take into account two subsequent trials i and $i+1$. To turn this procedure into the full ILO approach, two extensions are required. On the one hand, this is an initialization phase during the very first trial $i = 0$. This initialization consists of a classical (E)KF. On the other hand, it is necessary to correct the state estimates from trial to trial by storing the lumped correction term $\boldsymbol{\delta}_k^i$ as introduced in (2). Both extensions are straightforward and summarized in the structure diagram that is depicted in Fig. 1.

IV. Benchmark Example

A. Simplified Model of the Charging/ Discharging Dynamics of a Lithium-Ion Battery

As described, for example, in [13]–[15], equivalent circuit models can be used to approximate the charging/discharging dynamics of Lithium-Ion batteries. As depicted in Fig. 2, the associated state variables are then given by the normalized state of charge (SOC) $\sigma(t)$ as well as the voltages $v_{\mathrm{TL}}(t)$

Set $i = 0$, $k = 0$

While $k < k_{\max}$

- **Evaluate** the state prediction $\boldsymbol{\mu}_{k+1}^{\mathrm{p},0} = \mathbf{A}_k^0 \boldsymbol{\mu}_k^{\mathrm{e},0}$
- **Evaluate** the covariance prediction $\mathbf{C}_{k+1}^{\mathrm{p},0} = \mathbf{A}_k^0 \mathbf{C}_k^{\mathrm{e},0} \mathbf{A}_k^{0T} + \mathbf{E}_k^0 \mathbf{C}_{\mathbf{w},k} \mathbf{E}_k^{0T}$
- **Compute** the Kalman gain $\mathbf{H}_{1,k}^0$ according to the standard (E)KF procedure
- **Evaluate** the state update in the innovation step: $\boldsymbol{\mu}_k^{\mathrm{e},0} = \boldsymbol{\mu}_k^{\mathrm{p},0} + \mathbf{H}_{1,k}^0 \cdot \left(\mathbf{y}_{\mathrm{m},k}^0 - \mathbf{C}_k \boldsymbol{\mu}_k^{\mathrm{p},0}\right)$
- **Evaluate** the covariance update in the innovation step by the standard (E)KF procedure
- **Set** $k := k+1$

Set $\boldsymbol{\delta}_k^0 = \mathbf{0}$ for all $k \in \{0, \ldots, k_{\max}\}$

Store the measurement sequence $\mathbf{y}_{\mathrm{m},k}^0$

While $i < i_{\max}$

- **Set** $k = 0$
- **While** $k < k_{\max}$
  - **Evaluate** the state prediction
  $$\begin{bmatrix} \boldsymbol{\mu}_{k+1}^{\mathrm{p},i} \\ \boldsymbol{\mu}_{k+1}^{\mathrm{p},i+1} \end{bmatrix} = \begin{bmatrix} \mathbf{A}_k^i & \mathbf{0} \\ \mathbf{0} & \mathbf{A}_k^{i+1} \end{bmatrix} \cdot \begin{bmatrix} \boldsymbol{\mu}_k^{\mathrm{e},i} \\ \boldsymbol{\mu}_k^{\mathrm{e},i+1} \end{bmatrix} + \begin{bmatrix} \boldsymbol{\delta}_k^i \\ \boldsymbol{\delta}_k^i \end{bmatrix} \quad (22)$$
  including the disturbance estimate $\boldsymbol{\delta}_k^i$
  - **Evaluate** the covariance prediction according to Eq. (5)
  - **Compute** the optimal ILO gain acc. to Theorem 3.1
  - **Evaluate** the state and covariance update in the innovation step acc. to Eqs. (8) and (9)
  - **Set** $k := k+1$
- **Update** $\boldsymbol{\delta}_k^{i+1} = \left((i-1) \cdot \boldsymbol{\delta}_k^i + \mathbf{H}_{2,k}^{i+1} \cdot \left(\Delta \mathbf{y}_k^i - \Delta \mathbf{y}_k^{i+1}\right)\right) \cdot \frac{1}{i}$
- **Increment** the trial counter $i := i+1$
- **Store** the measurement sequence $\mathbf{y}_{\mathrm{m},k}^i$

Fig. 1: Structure diagram of the complete ILO algorithm.

and $v_{\mathrm{TS}}(t)$ across two RC sub-networks. These RC sub-networks represent processes with short and large time constants (TS and TL, respectively) due to electro-chemical polarization effects and concentration losses during charging and discharging. This model has been extended in [7] by a disturbance voltage $z(t)$ to represent effects such as aging and non-negligible temperature variations that affect the open-circuit voltage $v_{\mathrm{OC}}(\sigma(t))$. This extension is not further followed in the current paper, because we intend to estimate a model-mismatch by the additive disturbance variables $\boldsymbol{\delta}_k^i$ introduced in the previous sections, see Eq. (2) and Fig. 1.

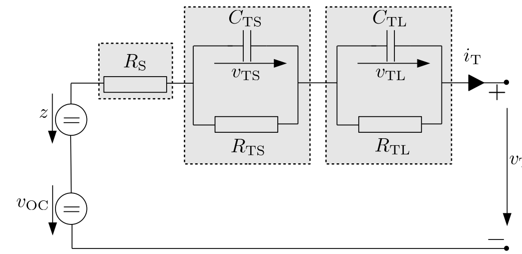

Fig. 2: Equivalent circuit model of a Lithium-Ion battery.

A continuous-time, quasi-linear model for the battery is given by

$$\begin{aligned} \dot{\mathbf{x}}(t) &= \mathbf{A}(\sigma(t)) \cdot \mathbf{x}(t) + \mathbf{b} \cdot u(t) \\ &= \begin{bmatrix} 0 & 0 & 0 & \frac{-1}{C_{\mathrm{Bat}}} \\ 0 & \frac{-1}{C_{\mathrm{TS}} \cdot R_{\mathrm{TS}}} & 0 & \frac{1}{C_{\mathrm{TS}}} \\ 0 & 0 & \frac{-1}{C_{\mathrm{TL}} \cdot R_{\mathrm{TL}}} & \frac{1}{C_{\mathrm{TL}}} \\ 0 & 0 & 0 & \frac{-1}{T_{\mathrm{I}}} \end{bmatrix} \cdot \mathbf{x}(t) + \begin{bmatrix} 0 \\ 0 \\ 0 \\ \frac{1}{T_{\mathrm{I}}} \end{bmatrix} \cdot u(t) \end{aligned} \quad (23)$$

with the state vector

$$\mathbf{x}(t) = \begin{bmatrix} \sigma(t) & v_{\mathrm{TS}}(t) & v_{\mathrm{TL}}(t) & i_{\mathrm{T}}(t) \end{bmatrix}^T \quad (24)$$

in which the measurable terminal current results from an underlying fast current controller. This underlying control loop leads to the first-order lag behavior ($T_{\mathrm{I}} = 0.1\,\mathrm{s}$)

$$T_{\mathrm{I}} \cdot \frac{\mathrm{d}i_{\mathrm{T}}(t)}{\mathrm{d}t} + i_{\mathrm{T}}(t) = i_{\mathrm{d}}(t) \quad (25)$$

for the temporal variation of the current $i_{\mathrm{T}}(t)$, where the system input $u(t) := i_{\mathrm{d}}(t)$ describes the corresponding set-point that is given by a periodically repeated trajectory.

Moreover, the first row of Eq. (23) comprises the integrating behavior

$$\dot{\sigma}(t) = -\frac{i_{\mathrm{T}}(t)}{C_{\mathrm{Bat}}} \quad (26)$$

between the terminal current and the normalized SOC $\sigma(t) \in [0\,;\,1]$, where $\sigma = 1$ denotes the fully charged battery with the capacitance C_{Bat}; the operating point $\sigma = 0$ then represents the completely discharged battery.

Although the terminal current $i_{\mathrm{T}}(t)$ is assumed to be measurable to demonstrate the proposed ILO scheme for a single-input multi-output scenario, the use of state estimators is inevitable to determine the true value of $\sigma(t)$. This is caused by the fact that neither its initial value $\sigma(0)$ nor the effective battery capacitance C_{Bat} are perfectly known in practice. Especially, the latter value depends strongly on the charging efficiency and on effects that can hardly be described in a model-based form such as aging and the influence of temperature variations. According to [13], [14], the state Eqs. (23) further describe variations of the voltages $v_\iota(t)$, $\iota \in \{\mathrm{TS}, \mathrm{TL}\}$, across both RC sub-networks

$$\dot{v}_\iota(t) = \frac{-v_\iota(t)}{C_\iota(t) \cdot R_\iota(t)} + \frac{i_\mathrm{T}(t)}{C_\iota(t)} \ . \tag{27}$$

The SOC dependencies of all equivalent circuit parameters have been identified experimentally in [16], in the form of

$$R_\mathrm{S}(t) = R_\mathrm{Sa} \cdot e^{R_\mathrm{Sb} \cdot \sigma(t)} + R_\mathrm{Sc} \tag{28}$$

for the Ohmic series resistance and by

$$R_\iota(t) = R_{\iota\mathrm{a}} \cdot e^{R_{\iota\mathrm{b}} \cdot \sigma(t)} + R_{\iota\mathrm{c}} \tag{29}$$

$$C_\iota(t) = C_{\iota\mathrm{a}} \cdot e^{C_{\iota\mathrm{b}} \cdot \sigma(t)} + C_{\iota\mathrm{c}} \ , \quad \iota \in \{\mathrm{TS}, \mathrm{TL}\} \tag{30}$$

for the parameters of the RC sub-networks. Note that the structure of these equations is based on the work of Erdinc et al. [13] and can be employed for a large variety of Lithium-Ion cells. Besides the terminal current $i_\mathrm{T}(t)$, also the battery's terminal voltage (derived by Kirchhoff's voltage law)

$$v_\mathrm{T}(t) = v_\mathrm{OC}(t) - v_\mathrm{TS}(t) - v_\mathrm{TL}(t) - i_\mathrm{T}(t) \cdot R_\mathrm{S}(t) \tag{31}$$

is available as a measured output, where the open-circuit voltage is described in the form

$$v_\mathrm{OC}(\sigma(t)) = v_0 \cdot e^{v_1 \cdot \sigma(t)} + \sum_{i=0}^{3} v_{i+2} \cdot \sigma^i(t) \ , \tag{32}$$

again by using the experimental parameter identification of [16]. To reformulate Eq. (32) into a quasi-linear form, the state-independent offset terms are subtracted from the expression for the open-circuit voltage so that the expression

$$\begin{aligned} \tilde{v}_\mathrm{OC}(\sigma(t)) &= \eta_\mathrm{OC}(\sigma(t)) \cdot \sigma(t) = v_\mathrm{OC}(\sigma(t)) - v_0 - v_2 \\ &= \left(v_0 \cdot \frac{e^{v_1 \cdot \sigma(t)} - 1}{\sigma(t)} + v_3 + v_4 \cdot \sigma(t) + v_5 \cdot \sigma^2(t) \right) \cdot \sigma(t) \end{aligned} \tag{33}$$

is obtained. In combination with the current measurement, this leads to the vector-valued output equation

$$\mathbf{y}(t) = \begin{bmatrix} i_\mathrm{T}(t) \\ \tilde{v}_\mathrm{T}(t) \end{bmatrix} = \begin{bmatrix} i_\mathrm{T}(t) \\ \tilde{v}_\mathrm{OC}(t) - v_\mathrm{TS}(t) - v_\mathrm{TL}(t) - i_\mathrm{T}(t) \cdot R_\mathrm{S}(t) \end{bmatrix} \tag{34}$$

with the quasi-linear representation

$$\begin{aligned} \mathbf{y}(t) &= \mathbf{C}(\sigma(t)) \cdot \mathbf{x}(t) \\ &= \begin{bmatrix} 0 & 0 & 0 & 1 \\ \eta_\mathrm{OC}(\sigma(t)) & -1 & -1 & -R_\mathrm{S}(t) \end{bmatrix} \cdot \mathbf{x}(t) \ . \end{aligned} \tag{35}$$

A temporally discretized version of this system model is obtained by the explicit Euler discretization

$$\mathbf{A}_k = \mathbf{I} + T \cdot \mathbf{A}(\sigma(t_k)) \tag{36}$$

with the sufficiently small step size T (here: $T = 10\,\mathrm{ms}$). In the output equation, the equality $\mathbf{C}_k = \mathbf{C}(\sigma(t_k))$ holds analogously. Effects of non-zero inputs are accounted for by adding the term

$$\mathbf{b}_k u_k = T \cdot \mathbf{b} \cdot u(t_k) \tag{37}$$

onto the formula (22) in the form

$$\begin{bmatrix} \boldsymbol{\mu}_{k+1}^{\mathrm{p},i} \\ \boldsymbol{\mu}_{k+1}^{\mathrm{p},i+1} \end{bmatrix} = \begin{bmatrix} \mathbf{A}_k^i & \mathbf{0} \\ \mathbf{0} & \mathbf{A}_k^{i+1} \end{bmatrix} \cdot \begin{bmatrix} \boldsymbol{\mu}_k^{\mathrm{e},i} \\ \boldsymbol{\mu}_k^{\mathrm{e},i+1} \end{bmatrix} + \begin{bmatrix} \mathbf{b}_k u_k \\ \mathbf{b}_k u_k \end{bmatrix} + \begin{bmatrix} \boldsymbol{\delta}_k^i \\ \boldsymbol{\delta}_k^i \end{bmatrix} \ . \tag{38}$$

Due to the fact that the input (37) is known (it is computed from the reference signal of the underlying current controller), and all imperfections with respect to the generation of the terminal current are summarized in the model mismatch $\boldsymbol{\delta}_k^i$ to be estimated, Eq. (38) is the only expression of the ILO algorithm of Fig. 1 that needs to be adjusted for the non-vanishing input considered in this example section.

B. Simulation Results of the ILO Approach

During the simulation-based evaluation of the ILO algorithm, two cases of a model-mismatch are considered:

Case 1 The true system, generating the measured data, has an additive offset $\begin{bmatrix} -10^{-8} & 0 & 10^{-4} & 0 \end{bmatrix}^T$ in comparison with the state Eqs. (23), representing errors in the magnitude of 0.02% wrt. the charging efficiency and up to 300% in the variation rates of the voltage v_TL.

Case 2 In addition to the error of **Case 1**, each element $A_{l,m,k}$ of $\mathbf{A}_k$ is disturbed by an independent time-invariant factor $1 + d_{l,m}$, where all $d_{l,m}$ are uniformly distributed random numbers from the interval $[0\,;\,0.1]$.

Assuming the true initial state $\mathbf{x}(0) = \begin{bmatrix} 0.65 & 0 & 0 & 0 \end{bmatrix}^T$ and the ILO initialization $\boldsymbol{\mu}_0^{\mathrm{e},0} = \begin{bmatrix} 0.78 & 0 & 0 & 0 \end{bmatrix}^T$ with $u(t) = 2\,\mathrm{A} \sin(2\pi t \cdot 3600\mathrm{s}^{-1})$ and $\mathbf{C}_{\mathbf{w},k} = 0.01^2\mathbf{I}$, $\mathbf{C}_{\mathbf{v},k} = \begin{bmatrix} 0.01 & 0 \\ 0 & 100 \end{bmatrix}$, the estimation results in Figs. 3 and 4 are obtained. It can be clearly seen that the ILO is capable in both considered cases to reduce the root mean square errors (computed along the complete trial) by around 20% in the SOC and the voltage v_TL after the 2nd or 3rd trial. These variables are those states that have the largest absolute estimation errors in **Case 1**. This improvement is confirmed for **Case 2**, however, with larger remaining errors in the directly measured terminal current which still remain below the measurement's standard deviation.

V. Conclusions and Outlook on Future Work

In this paper, a novel stochastic ILO has been derived for linear time-varying systems so that the estimation covariance is minimized. Future work will aim at incorporating physically inspired disturbance models replacing the model-free term $\boldsymbol{\delta}_k^i$ to provide the basis for an iterative parameter identification, for fault detection and isolation, as well as for including the ILO in closed-loop control structures.

References

[1] S. Arimoto, S. Kawamura, and F. Miyazaki, "Bettering Operations of Robots by Learning," *Journal of Robotic Systems*, vol. 1, no. 1, pp. 123–140, 1984.

[2] H. S. Ahn, Y. Chen, and K. L. Moore, "Iterative Learning Control: Brief Survey and Categorization," *IEEE Transactions on Systems, Man and Cybernetics, Part C*, vol. 37, no. 6, pp. 1109–1121, 2007.

[3] D. A. Bristow, M. Tharayil, and A. G. Alleyne, "A survey of iterative learning control: A learning-based method for high-performance tracking control," *IEEE Control Systems Magazine*, vol. 26, no. 3, pp. 96–114, 2006.

[4] J. Hatonen and K. L. Moore, "A New Arimoto-Type Algorithm to Estimate States for Repetitive Processes: Iterative Learning Observer (ILO)," in *Proc. of 22nd Intl. Symposium on Intelligent Control*, Singapore, 2007, pp. 232–236.

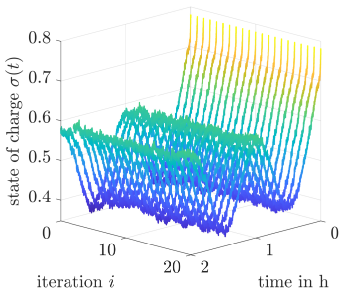

(a) Estimation of the SOC σ.

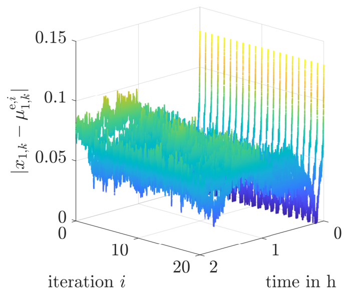

(b) Estimation error of the SOC σ.

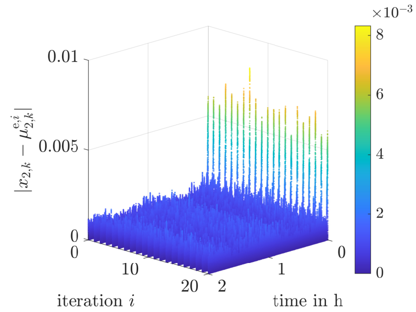

(c) Estimation error of the voltage v_{TS}.

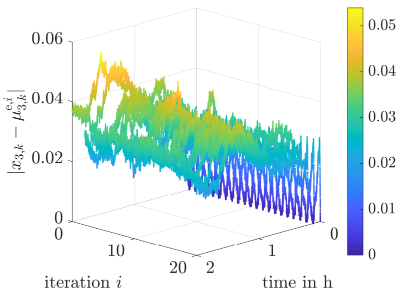

(d) Estimation error of the voltage v_{TL}.

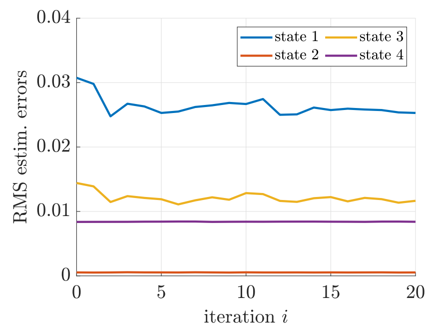

(e) Root mean square estimation errors.

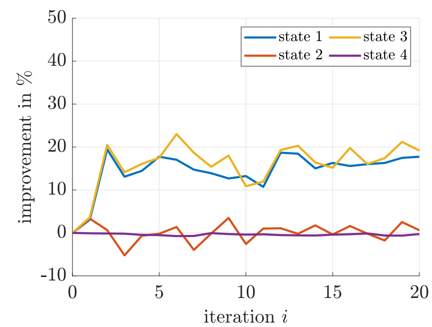

(f) Improvement of the estimates by the ILO.

Fig. 3: Estimation results of the stochastic ILO in the **Case 1**.

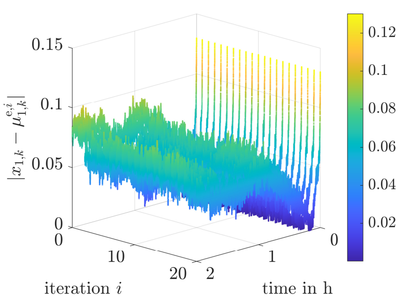

(a) Estimation error of the SOC σ.

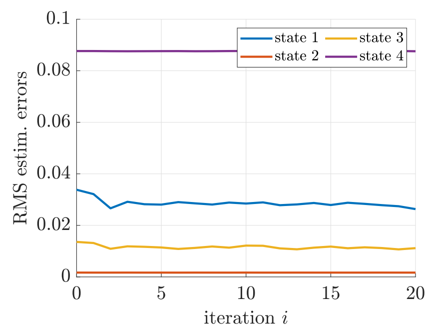

(b) Root mean square estimation errors.

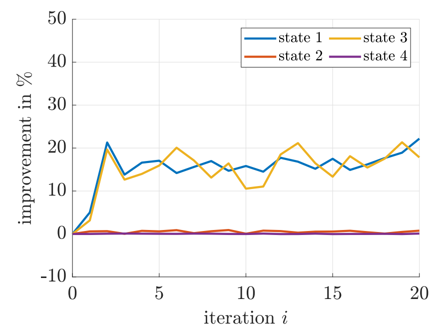

(c) Improvement of the estimates by the ILO.

Fig. 4: Estimation results of the stochastic ILO in the **Case 2**.

[5] Z. Cao, J. Lu, R. Zhang, and F. Gao, "Iterative Learning Kalman Filter for Repetitive Processes," *Journal of Process Control*, vol. 46, pp. 92–104, 2016.

[6] R. Kalman, "A New Approach to Linear Filtering and Prediction Problems," *Transaction of the ASME – Journal of Basic Engineering*, vol. 82, no. Series D, pp. 35–45, 1960.

[7] A. Rauh, J. Kersten, and H. Aschemann, "Iterative Learning Approaches for Discrete-Time State and Disturbance Observer Design of Uncertain Linear Parameter-Varying Systems," in *Proc. of the 8th IFAC Symposium on Mechatronic Systems MECHATRONICS 2019*, Vienna, Austria, 2019.

[8] W. Chen and M. Saif, "An Iterative Learning Observer-Based Approach to Fault Detection and Accommodation in Nonlinear Systems," in *Proc. of the 40th IEEE Conference on Decision and Control*, vol. 5, Orlando, FL, USA, 2001, pp. 4469–4474.

[9] A. Chakrabarty, A. Zemouche, R. Rajamani, and M. Benosman, "Robust Data-Driven Neuro-Adaptive Observers With Lipschitz Activation Functions," in *Proc. of the 58th Conference on Decision and Control (CDC)*, Nice, France, 2019, pp. 2862–2867.

[10] A. Chakrabarty and M. Benosman, "Safe Learning-based Observers for Unknown Nonlinear Systems using Bayesian Optimization," 2021, https://arxiv.org/abs/2005.05888.

[11] T. Chevet, A. Rauh, T. N. Dinh, J. Marzat, and T. Raïssi, "Robust Interval Observer for Systems Described by the Fornasini-Marchesini Second Model," *IEEE Control Systems Letters*, vol. 6, pp. 1940–1945, 2022.

[12] A. Papoulis, *Probability, Random Variables, and Stochastic Processes*. New York: McGraw-Hill, 1991.

[13] O. Erdinc, B. Vural, and M. Uzunoglu, "A Dynamic Lithium-Ion Battery Model Considering the Effects of Temperature and Capacity Fading," in *Proceedings of International Conference on Clean Electrical Power*, 2009, pp. 383–386.

[14] A. Rauh, S. Butt, and H. Aschemann, "Nonlinear State Observers and Extended Kalman Filters for Battery Systems," *International Journal of Applied Mathematics and Computer Science AMCS*, vol. 23, no. 3, pp. 539–556, 2013.

[15] L. Senkel, A. Rauh, and H. Aschemann, "Robust Procedures for the Estimation of Operating Conditions of Lithium-Ion Battery Cells," in *Proc. of 2nd Intl. Conference on Control and Fault-Tolerant Systems (SysTol)*, Nice, France, 2013.

[16] J. Reuter, E. Mank, H. Aschemann, and A. Rauh, "Battery State Observation and Condition Monitoring Using Online Minimization," in *Proc. of 21st Intl. Conference on Methods and Models in Automation and Robotics*, Miedzyzdroje, Poland, 2016.